Inorganic Chemistry

Article

pubs.acs.org/IC

Selectivity of the Highly Preorganized Tetradentate Ligand 2,9-Di(pyrid-2-yl)-1,10-phenanthroline for Metal Ions in Aqueous Solution, Including Lanthanide(III) Ions and the Uranyl(VI) Cation

Ashley N. Carolan,[†] Gregory M. Cockrell,[†] Neil J. Williams,[†] Gang Zhang,[‡] Donald G. VanDerveer,[§] Hee-Seung Lee,[†] Randolph P. Thummel,*[,‡] and Robert D. Hancock.*[,†]

[†]Department of Chemistry and Biochemistry, University of North Carolina Wilmington, Wilmington, North Carolina 28403, United States

[‡]Department of Chemistry, University of Houston, Houston, Texas 77004, United States

[§]Department of Chemistry, Clemson University, Clemson, South Carolina 29634, United States

Supporting Information

ABSTRACT: Some metal ion complexing properties of DPP (2,9-Di(pyrid-2-yl)-1,10-phenanthroline) are reported with a variety of Ln(III) (Lanthanide(III)) ions and alkali earth metal ions, as well as the uranyl(VI) cation. The intense $\pi-\pi^*$ transitions in the absorption spectra of aqueous solutions of 10^{-5} M DPP were monitored as a function of pH and metal ion concentration to determine formation constants of the alkali-earth metal ions and Ln(III) (Ln = lanthanide) ions. It was found that log K_1(DPP) for the Ln(III) ions has a peak at Ln(III) = Sm(III) in a plot of log K_1 versus $1/r^+$ (r^+ = ionic radius for 8-coordination). For Ln(III) ions larger than Sm(III), there is a steady rise in log K_1 from La(III) to Sm(III), while for Ln(III) ions smaller than Sm(III), log K_1 decreases slightly to the smallest Ln(III) ion, Lu(III). This pattern of variation of log K_1 with varying size of Ln(III) ion was analyzed using MM (molecular mechanics) and DFT (density functional theory) calculations. Values of strain energy ($\sum$U) were calculated for the $[Ln(DPP)(H_2O)_5]^{3+}$ and $[Ln(qpy)(H_2O)_5]^{3+}$ (qpy = quaterpyrdine) complexes of all the Ln(III) ions. The ideal M−N bond lengths used for the Ln(III) ions were the average of those found in the CSD (Cambridge Structural Database) for the complexes of each of the Ln(III) ions with polypyridyl ligands. Similarly, the ideal M−O bond lengths were those for complexes of the Ln(III) ions with coordinated aqua ligands in the CSD. The MM calculations suggested that in a plot of $\sum$U versus ideal M−N length, a minimum in $\sum$U occurred at Pm(III), adjacent in the series to Sm(III). The significance of this result is that (1) MM calculations suggest that a similar metal ion size preference will occur for all polypyridyl-type ligands, including those containing triazine groups, that are being developed as solvent extractants in the separation of Am(III) and Ln(III) ions in the treatment of nuclear waste, and (2) Am(III) is very close in M−N bond lengths to Pm(III), so that an important aspect of the selectivity of polypyridyl type ligands for Am(III) will depend on the above metal ion size-based selectivity. The selectivity patterns of DPP with the alkali-earth metal ions shows a similar preference for Ca(II), which has the most appropriate M−N lengths. The structures of DPP complexes of Zn(II) and Bi(III), as representative of a small and of a large metal ion respectively, are reported. $[Zn(DPP)_2](ClO_4)_2$ (triclinic, $P1$, R = 0.0507) has a six-coordinate Zn(II), with each of the two DPP ligands having one noncoordinated pyridyl group appearing to be π-stacked on the central aromatic ring of the other DPP ligand. $[Bi(DPP)(H_2O)_2(ClO_4)_2](ClO_4)$ (triclinic, $P1$, R = 0.0709) has an eight-coordinate Bi, with the coordination sphere composed of the four N donors of the DPP ligand, two coordinated water molecules, and the O donors of two unidentate perchlorates. As is usually the case with Bi(III), there is a gap in the coordination sphere that appears to be the position of a lone pair of electrons on the other side of the Bi from the DPP ligand. The Bi-L bonds become relatively longer as one moves from the side of the Bi containg the DPP to the side where the lone pair is thought to be situated. A DFT analysis of $[Ln(tpy)(H_2O)_n]^{3+}$ and $[Ln(DPP)(H_2O)_5]^{3+}$ complexes is reported. The structures predicted by DFT are shown to match very well with the literature crystal structures for the $[Ln(tpy)(H_2O)_n]^{3+}$ with Ln = La and n = 6, and Ln = Lu with n = 5. This then gives one confidence that the structures for the DPP complexes generated by DFT are accurate. The structures generated by DFT for the $[Ln(DPP)(H_2O)_5]^{3+}$ complexes are shown to agree very well with those generated by MM, giving one confidence in the accuracy of the latter. An analysis of the DFT and MM structures shows the decreasing O--O nonbonded distances as one progresses from La to Lu, with these distances being much less than the sum of the van der Waals radii for the smaller Ln(III) ions. The effect that such short O--O nonbonded distances has on thermodynamic complex stability and coordination number is then discussed.

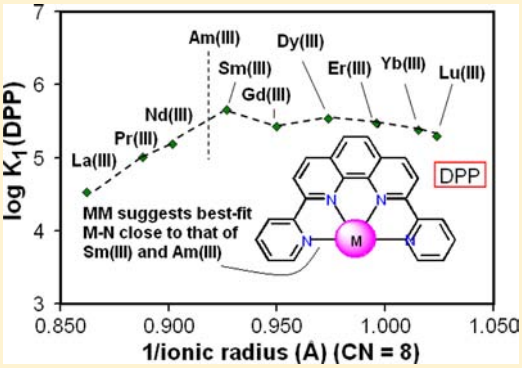

Received: February 2, 2012
Published: December 11, 2012

dx.doi.org/10.1021/ic3002509 | *Inorg. Chem.* 2013, 52, 15−27

INTRODUCTION

Ligands such as DPP[1] (see Figure 1 for key to ligand abbreviations) are of considerable interest because of the potential use of

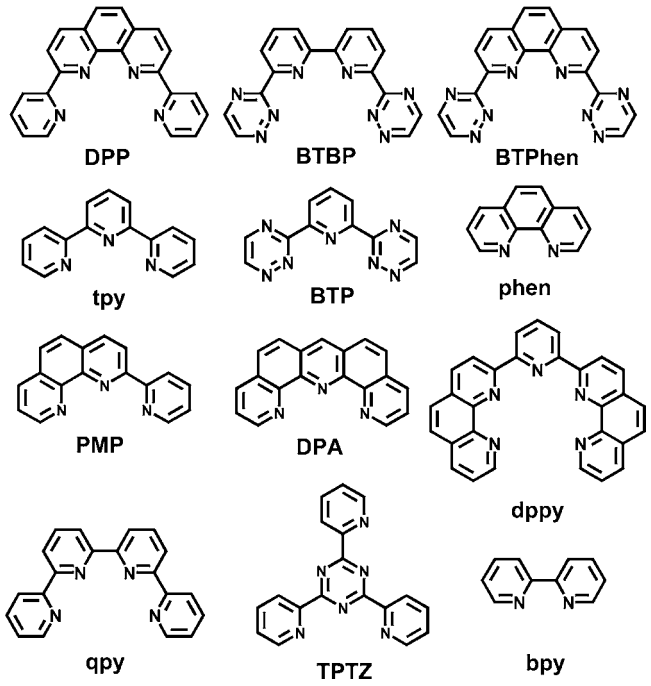

Figure 1. Ligands discussed in this paper.

heterocyclic aromatic ligands such as BTP[2] or BTPhen[3] as the basis for solvent extractants for the separation of Am(III) from Ln(III) (Ln = lanthanide) ions, particularly Gd(III), in the treatment of nuclear waste. The separation of Am(III) from Ln(III) ions depends on the greater tendency toward covalent bonding in Am(III) than the Ln(III) ions,[4,5] which indicates the use of more covalent M−N (metal−nitrogen) bonding ligands such as BTBP or BTPhen. The logic in the use of BTPhen rather than BTBP was the higher level of preorganization[6] afforded by the reinforcing benzo group of BTPhen, paralleling the thermodynamically more stable complexes formed by DPA[7] than tpy.[8] A preorganized ligand is one which is constrained to be in, or close to, the conformation required to complex the target metal ion.[6] In the case of the preorganization afforded by reinforcing benzo groups, the amount of accompanying thermodynamic stabilization and its origin are clear.[9,10] Free ligands such as bpy, tpy, or qpy have the N-donors in a *trans* conformation, and, as calculated by DFT in simulated aqueous solution,[10] an energy of 1.6 kcal mol^{-1} is required to rotate the pyridyl groups of bpy into the *cis* conformation required to complex the metal ion. In contrast, phen is locked by its reinforcing benzo group into a *cisoid* conformation, and so does not have to overcome this unfavorable contribution to the thermodynamic stability of its complexes. The log K_1 values of complexes of phen are thus found to be a fairly constant 1.3 log units higher than log K_1 for bpy with the same metal ion.[9,10] The study of ligands such as DPA,[7] tpy,[8] MPP,[11] diphen,[12] or DPP[1] coupled with known[13] formation constants for the simpler analogues bpy and phen has begun to reveal a pattern in the formation constants (log K_1) of these ligands governed by the number of pyridyl donors, and the number of reinforcing benzo groups, illustrated in Scheme 1.

What appears to be a systematic increase in log K_1 for Ca(II) with increasing numbers of pyridyl donors and reinforcing benzo groups leads one to speculate on what high log K_1 value might be obtained for Ca(II) with a ligand such as dppy in Figure 1, which we are currently studying. It appears from Scheme 1 that for Ca(II), each addition of a pyridyl donor to ligands with equal levels of preorganization increases log K_1 by about 1.3 log units, and each additional reinforcing benzo group increases log K_1 also by about 1.3 log units, because of preorganization as outlined above.[9,10] One might predict on this basis that log K_1 for Ca(II) with dppy, which has 5 pyridyl donors and two reinforcing benzo groups, should be about 6.5, the largest log K_1 for Ca(II) with[13] any purely N-donor ligand.

The increased preorganization provided by increasing numbers of benzo groups in the ligands in Scheme 1 increases log K_1 only for large metal ions, that is, those having an ionic radius[15] (r^+) of close to 1.0 Å. This can be understood in terms of the rule[9] that five-membered chelate rings, as are present in the ligands in Scheme 1, favor coordination with large metal ions, while six-membered chelate rings such as are present in DPN (Scheme 2) favor very small Lewis acids of the size of Be^{2+} (r^+ = 0.27 Å[15]) or B(III) (r^+ = 0.11 Å[15]).

Thus, log K_1 increases markedly, for example, for the large Ca(II) (r^+ = 1.00 Å[15]) and Ln(III) ions (r^+ = 1.03 Å[15]) in passing from tpy[8] to DPA.[7] Small metal ions such as Mg(II) or Zn(II),[15] are not well accommodated by five-membered chelate rings.[9] Thus, the increase in log K_1 in passing from tpy to the more rigid DPA, which rigidity exacerbates the problem of accommodating to five-membered chelate rings, is small.[7,8] It is of considerable interest that the structure of a B(III) complex of DPN,[16] and of a Pt(II) complex of 3,8-dichloro-DPN,[17] have been reported. As expected from Scheme 2, the very small B(III) with its B−N bond lengths[16] to DPN of 1.507 Å is close to a best-fit size for DPN, and the B(III) lies in the plane of the DPN ligand, and there is very little sign of steric distortion of the DPN or the coordination geometry of the B(III). In contrast, Pt(II) has Pt−N bond lengths of 2.024 Å, which may not seem to greatly exceed the best-fit M−N length for coordinating with DPN in Scheme 2, but the structure shows a strongly bowed ligand with the too-large Pt(II) lying well out of the ligand plane because of its poor fit into the cleft of the dichloro-DPN.[17]

In this paper the effect of the size selectivity expected from DPP on the log K_1 values for a selection of Ln(III) ions from La(III) to Lu(III) is reported. The alkali earth metal ions present a range of ionic radii[15] from the small Mg(II) ion (r^+ = 0.74 Å), the large Ca(II) (r^+ = 1.0 Å) and Sr(II) (r^+ = 1.18 Å) ions, to the very large Ba(II) ion (r^+ = 1.36 Å), so that these are studied here also to see how these size variations affect complex stability. The pattern of selectivity of Ln(III) ions for DPP and other polypyridyl ligands prompted us to undertake a MM (molecular mechanics) investigation of the best-fit size of Ln(III) ion for these ligands. MM offers an important advantage[18] over otherwise more powerful approaches such as DFT[10,19−23] to understanding metal ion selectivity, in that it can isolate purely steric effects, and so give insights into steric factors controlling metal ion selectivity. In addition, the stability of the complex of UO_2^{2+} with DPP in aqueous solution is investigated. The UO_2^{2+} cation is a fairly acidic metal ion.[13] This high acidity makes study of its complexes with purely N donor ligands difficult because of a tendency to hydrolyze to yield precipitates of the hydroxides rather than formation of the intended N donor complex in aqueous solution. The higher levels of preorganization of DPP might lead to complexes of UO_2^{2+} stable enough to resist hydrolysis, which would lead to new insights on the affinity of the uranyl(VI) cation for N-donor ligands.

dx.doi.org/10.1021/ic3002509 | *Inorg. Chem.* 2013, 52, 15−27

Scheme 1. Effect of Number of Pyridyl Donor Groups and Level of Preorganization Provided by Varying Numbers of Reinforcing Benzo Groups on Formation Constants (log K_1) of the Ca(II) Complexes in Aqueous Solution[1,7,8,11−14]

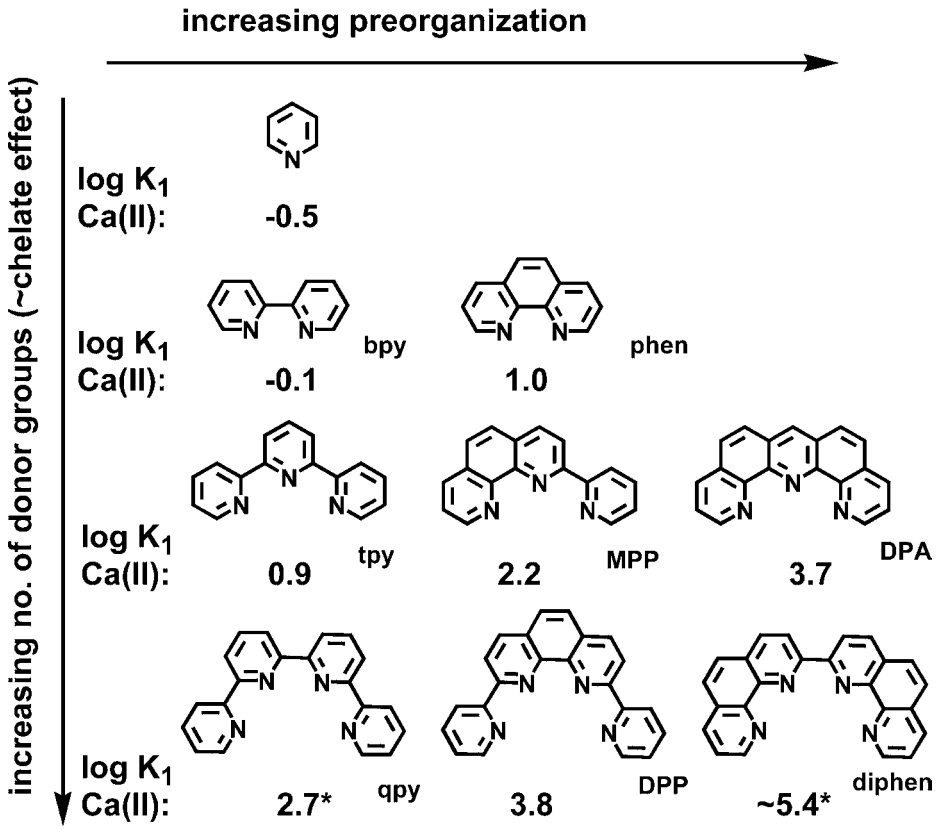

*50% MeOH.

Scheme 2. Best-Fit M−N Lengths for Metal Ions Coordinating in (a) the Five-Membered Chelate Ring Formed by phen, or (b) the Six-Membered Ring Formed by DPN

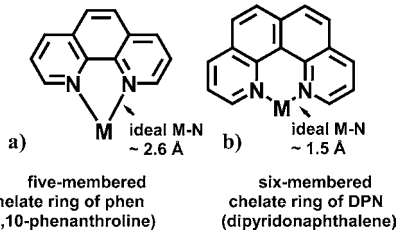

A main focus of this paper is the size-based selectivity produced by the rigid DPP ligand. The structures are reported of the small Zn(II) ion (r^+ = 0.74 Å) complex with DPP and the large Bi(III) (r^+ = 1.03 Å) complex with DPP, to add some insights into how metal ions adapt to the best-fit size preferences of DPP. An attempt was made to grow crystals of the Ln(III) ions of the $[Ln(L)(H_2O)_n]Cl_3$ type (L = qpy or DPP, n = 4 or 5), which should contain complex cations of the $[Ln(L)(H_2O)_n]^{3+}$ type, resembling the complexes expected to be present in aqueous solution, but with no success. The Cl^- ion is the preferred counterion, as other counterions such as NO_3^- or ClO_4^- invariably displace waters and coordinate to the Ln(III) cation,[24] whereas in complexes of the type $[Ln(tpy)(H_2O)_n]Cl_3$ the Cl^- anions do not coordinate.[25] Structures have been reported[26,27] for the $[Y(qpy)(NO_3)_2(H_2O)_4]^+$ and $[Eu(DPP)_2H_2O]^{3+}$ cations, which, however, do not allow for direct comparison with the MM calculations reported here. In lieu of being able to grow crystals containing complex cations of the $[Ln(L)(H_2O)_5]^{3+}$ type (L = DPP and qpy), DFT calculations are reported here on $[Ln(L)(H_2O)_n]^{3+}$ complexes for Ln = La(III) and Lu(III), L = DPP, n = 5, and L = tpy, with n = 5 and 6.

EXPERIMENTAL SECTION

Materials. DPP was synthesized following a previously reported method.[28] The metal perchlorates were obtained from VWR and Alfa-Aesar, either as the crystalline salts or, in the case of many of the Ln(III) perchlorates, as 50% w/w aqueous solutions of the salts, which were used as received. The solids, or 50% solutions, were used to prepare stock solutions of the metal perchlorates that were close to 0.05 M, and these stock solutions were then standardized by EDTA titration.[29] Stock solutions of the more hydrolysis prone metal ion UO_2^{2+} were prepared from the nitrate salts at pH 2.0. All solutions were made up in deionized water (Milli-Q, Waters Corp.) of >18 MΩ cm^{-1} resistivity.

Synthesis of Complexes of DPP. The general procedure followed for the synthesis of Zn(II) and Bi(III) complexes with DPP was as follows. One equivalent of DPP (about 10 mg) was dissolved in n-butanol (20 mL) and one equivalent of the metal perchlorate was dissolved in deionized water (20 mL). The aqueous solution of the metal perchlorate was placed in a 50 mL beaker, and the n-butanol solution of DPP was carefully layered on top of the water layer. The beaker was covered with parafilm, and then left to stand. After a few days, crystals of the DPP complex formed at the interface of the solvents, and some crystals began to fall to the bottom of the beaker. The solutions were filtered under vacuum, and air-dried.

*$[Zn(DPP)_2](ClO_4)_2$ (**1**).* Colorless crystals. Elemental analysis, calculated for $C_{44}H_{28}Cl_2N_8O_8Zn$: C, 56.64; H, 3.02; N 12.01%. Found: C, 56.41; H, 2.91; N, 11.89%.

dx.doi.org/10.1021/ic3002509 | Inorg. Chem. 2013, 52, 15−27

*[Bi(DPP)(H$_2$O)$_2$(ClO$_4$)$_2$](ClO$_4$) (**2**).* Colorless crystals. Elemental analysis, calculated for $C_{22}H_{18}BiCl_3N_4O_{14}$: C, 30.10; H, 2.07; N 6.38%. Found: C, 30.43; H, 2.46; N, 6.35%.

Molecular Structure Determination. A Rigaku Mercury diffractometer, using the omega scan mode, was employed for crystal screening, unit cell determination, and data collection. The structure was solved by direct methods, and refined to convergence.[30] Some details of the structure determination are given in Table 1, and crystal coordinates

Table 1. Crystal Data and Details of Structure Refinement for [Zn(DPP)$_2$](ClO$_4$)$_2$ (1) and [Bi(DPP)(H$_2$O)$_2$(ClO$_4$)$_2$]-(ClO$_4$) (2)

	1	2
empirical formula:	$C_{44}H_{28}Cl_2N_8O_8Zn$	$C_{22}H_{18}BiCl_3N_4O_{14}$
formula weight:	933.01	877.73
temperature (K)	153(2)	153(2)
wavelength (Å):	0.71073	0.71073
crystal system:	triclinic	triclinic
space group:	*P*1	*P*1
unit cell dimensions:		
a (Å)	7.8346(16)	9.0538(10)
b (Å)	10.333(2)	9.0953(8)
c (Å)	23.502(5)	17.3130(14)
α (deg)	79.51(3)	79.480(15)
β (deg)	80.43(3)	80.320(14)
γ (deg)	76.10(3)	72.610(13)
volume (Å^3):	1801.1(6)	1327.8(2)
Z	2	2
final R indices [$I > 2\sigma(I)$]	*R*1 = 0.0507	*R*1 = 0.0709
	*wR*2 =0.0679	*wR*2 = 0.1722
R indices (all data)	*R*1 = 0.0950	*R*1 = 0.0882
	*wR*2 =0.1062	*wR*2 = 0.1914

and details of the structure determination of **1** and **2** have been deposited with the CSD (Cambridge Structural Database).[24] A selection of bond lengths and angles for **1** and **2** are given in Tables 2−3. The structures of **1** and **2** are shown in Figures 9 and 10.

Table 2. Selected Bond Lengths (Å) and Angles (deg) in [Zn(DPP)$_2$](ClO$_4$)$_2$ (1)

	Lengths (Å)		
Zn(1)−N(1)	2.125(5)	Zn(1)−N(2)	2.067(5)
Zn(1)−N(5)	2.263(5)	Zn(1)−N(6)	2.057(5)
Zn(1)−N(3)	2.133(5)	Zn(1)−N(7)	2.217(5)
	Angles (deg)		
N(1)−Zn(1)−N(2)	74.8(2)	N(2)−Zn(1)−N(3)	74.4(2)
Zn(1)−N(1)−C(5)	112.2(4)	Zn(1)−N(2)−C(6)	121.6(4)
N(2)−Zn(1)−N(6)	161.6(2)	Zn(1)−N(2)−C(14)	120.8(4)
Zn(1)−N(3)−C(13)	111.3(4)	Zn(1)−N(3)−C(17)	125.6(4)

Formation Constant Determination. We have recently[7,8] developed improved techniques for preparing solutions of ligands of low water solubility. Direct dissolution of DPP in acidic aqueous solutions with 0.1 M NaClO$_4$ present to generate a constant ionic strength (μ) yielded[1] truly dissolved solutions of at most 4×10^{-6} M. Dissolution is judged to be complete because of the absence of intense light scattering peaks in the vicinity of 200 nm. The improved technique involves preparing a 10^{-3} M stock solution of DPP in MeOH, and then using this to prepare 10^{-5} M solutions of DPP in water. It was found that to obtain spectra with no light scattering, it was best to let the stock solution of DPP in MeOH stand for a few days. The 1% of MeOH in the aqueous solutions prepared from the stock solution of DPP in MeOH is considered[7,8] to have a negligible effect. A further important aspect in promoting solubility of ligands such as DPP is the omission of a

Table 3. Selected Bond Lengths (Å) and Angles (deg) in [Bi(DPP)(H$_2$O)$_2$(ClO$_4$)$_2$](ClO$_4$) (2)

	Lengths (Å)		
Bi(1)−O(1)	2.383(11)	Bi(1)−O(2)	2.337(12)
Bi(1)−O(7)	2.787(11)	Bi(1)−N(1)	2.529(11)
Bi(1)−N(3)	2.407(11)	Bi(1)−N(4)	2.523(11)
Bi(1)−O(3)	2.739(11)	Bi(1)−N(2)	2.417(11)
	Angles (deg)		
N(2)−Bi(1)−N(1)	65.6(4)	N(3)−Bi(1)−N(2)	68.8(4)
N(3)−Bi(1)−N(4)	65.9(4)	O(1)−Bi(1)−N(1)	95.4(4)
O(1)−Bi(1)−N(2)	79.9(4)	C(5)−N(1)−Bi(1)	119.1(9)
C(1)−N(1)−Bi(1)	120.9(9)	C(6)−N(2)−Bi(1)	121.4(9)
C(14)−N(2)−Bi(1)	116.4(8)	N(2)−C(6)−C(5)	117.4(12)

background electrolyte, which is usually added to control μ. It was found[7,8] that addition of salts such as NaCl or NaClO$_4$ to control μ salted out these marginally soluble ligands. Since the DPP is present at 10^{-5} M and metal ion salts and acids or bases used in the titrations are also present only at low concentrations, the effective value of μ is zero.

UV−visible spectra were recorded using a Varian 300 Cary 1E UV−visible Spectrophotometer controlled by Cary Win UV Scan Application version 02.00(5) software. A VWR sympHony SR60IC pH meter with a VWR sympHony gel epoxy semimicro combination pH electrode was used for all pH readings, which were made in the external titration cell, with N_2 bubbled through the cell to exclude CO_2. The pH meter was calibrated using standard acid−base titration methods, in which $E°$ for the cell was determined from a linear plot of E vs calculated pH.

The log K_1 values determined for Ln(III) and alkali earth cations were obtained by titration of 10^{-5} M solutions of DPP with solutions of the metal perchlorates. The pH was initially adjusted to about 5.0, which gives a higher concentration of free ligand, and is lower than the region where hydrolysis of the Ln(III) ions occurs. It is thus not necessary to correct for such hydrolysis. The pH was monitored through the course of the titration, and these pH values, which changed little during the course of the titration, were incorporated into the calculation of the free ligand concentration as controlled by the previously measured pK_a values of the ligand. The spectra of 10^{-5} M solutions of DPP titrated with Ca(ClO$_4$)$_2$ and Pr(ClO$_4$)$_3$ solutions are shown in Figures 2a and 3 respectively. The resulting variation in absorption at five different wavelengths was analyzed as a function of metal ion concentration using Excel.[32] The variation of absorption at different wavelengths as a function of log [Ca^{2+}] is seen in Figure 2b. The solid lines are theoretical curves fitted simultaneously to all five wavelengths using the Solver module of Excel, and the empirically fitted value of log K_1 for the Ca(II)/DPP complex plus molar absorbtivities of the free DPP ligand plus the Ca(II)/DPP complex. The log K_1 values for DPP with the UO_2^{2+} cation were obtained by titrating a 10^{-5} M solution of DPP and of UO$_2$(NO$_3$)$_2$ over the pH range 2.70 to 5.38, as seen in Figure 8a. This different approach was taken because of the acidity of the UO_2^{2+} cation, which would not allow for free UO_2^{2+} cation solutions at a pH high enough to be used for titrating the DPP ligand solutions. The standard deviations given for the equilibrium constants for DPP in Table 4 were calculated using the Solvstat macro provided with reference 32, and relate to the overall goodness of fit for all five wavelengths.

Molecular Mechanics Calculations. The program HyperChem[33] was used for MM (molecular mechanics) calculations. HyperChem allows one to add force-field parameters, and so ideal M−N lengths involving pyridyl groups with Ln(III) ions, and ideal M−O lengths involving coordinated water molecules were obtained from the CSD.[24] These ideal bonds are given in Table 5. The M−N and M−O force constants were set at 0.7 mdyne Å^{-1}, which has been found[34] to give satisfactory results in calculating curves of steric strain as a function of M−L (metal−ligand) bond length, as seen for [Ln(qpy)(H$_2$O)$_5$]$^{3+}$ and [Ln(DPP)(H$_2$O)$_5$]$^{3+}$ complexes in Figure 5.

Density Functional Theory (DFT) Calculations. All DFT calculations reported in this work were carried out with the ab initio quantum chemistry package GAMESS.[35] Geometry optimization of the Ln(III)/polypyridyl complexes was performed within the framework of

dx.doi.org/10.1021/ic3002509 | *Inorg. Chem.* 2013, 52, 15−27

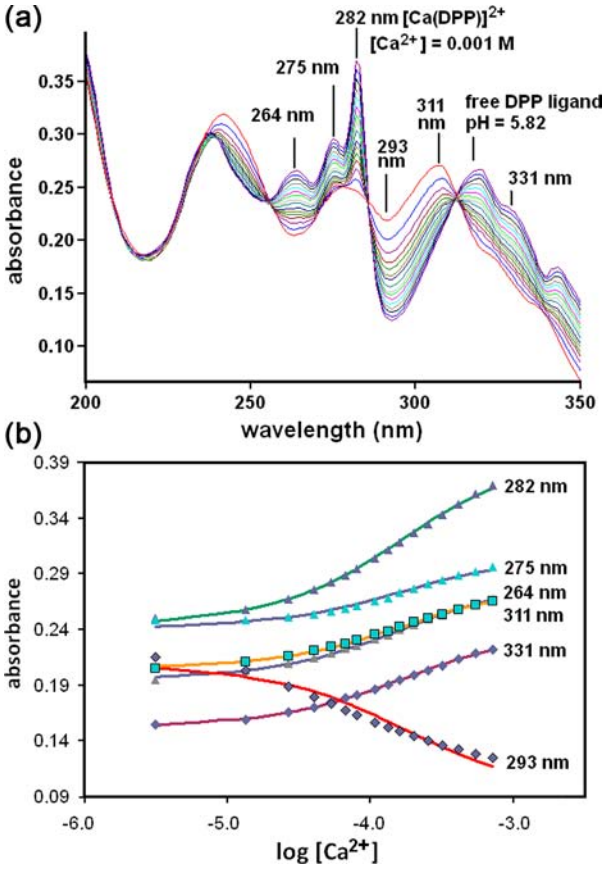

Figure 2. (a) Spectra of DPP (10^{-5} M) in aqueous solution at pH 5.82 at a variety of Ca^{2+} concentrations, 25 °C, $\mu = 0$. The Ca^{2+} concentrations range from no added Ca^{2+} to 0.001 M Ca^{2+}, where the Ca(II)/DPP complex is close to fully formed. The wavelengths indicated are those used in fitting log K_1(DPP) for the Ca(II) complex, as shown in panel b. (b) Variation of absorbance at six different wavelengths of 10^{-5} M DPP aqueous solutions as a function of log [Ca^{2+}]. The points are experimental values, whereas the solid lines are theoretical curves fitted to the experimental data using Solver,[18] log K_1(DPP) for Ca^{2+} = 3.77, and fitted values of the molar absorbtivities of free DPP ligand and the Ca(II)/DPP complex.

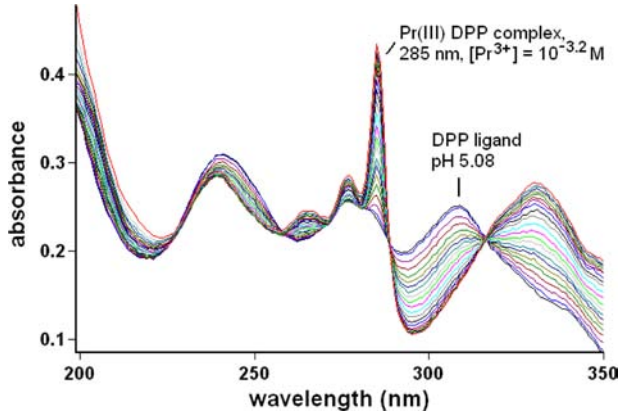

Figure 3. Spectra of DPP (10^{-5} M) in aqueous solution at pH 5.08 at a variety of Pr^{3+} concentrations, 25 °C, $\mu = 0$. The Pr^{3+} concentrations range from no added Pr^{3+}, where the free DPP ligand plus a fraction of monoprotonated DPP is present, to 0.0006 M Pr^{3+}, where the Pr(III)/DPP complex is fully formed.

Kohn–Sham DFT with B3LYP exchange-correlation functional.[36,37] The SV(P) basis set[38] was used for the main group elements, whereas the effective core potential of Stevens-Cundari[39] (SBKJC in GAMESS) was used for the Ln(III) ions. All DFT calculations were performed in an aqueous solution environment using a polarizable continuum model (PCM) as implemented in GAMESS.

Table 4. Protonation and Formation Constants Determined for DPP (L) at 25 °C and Ionic Strength (μ) = 0

equilibrium	log K
$H^+ + OH^- \leftrightarrows H_2O$	13.78[a]
$L + H^+ \leftrightarrows LH^+$	4.41(3)
$LH^+ + H^+ \leftrightarrows LH_2^{2+}$	3.14(2)
$Mg^{2+} + L \leftrightarrows MgL^{2+}$	0.7(1)
$Ca^{2+} + L \leftrightarrows CaL^{2+}$	3.77(4)
$Sr^{2+} + L \leftrightarrows SrL^{2+}$	2.38(2)
$Ba^{2+} + L \leftrightarrows BaL^{2+}$	1.43(5)
$La^{3+} + L \leftrightarrows LaL^{3+}$	4.52(2)
$Pr^{3+} + L \leftrightarrows PrL^{3+}$	5.01(2)
$Nd^{3+} + L \leftrightarrows NdL^{3+}$	5.19(3)
$Sm^{3+} + L \leftrightarrows SmL^{3+}$	5.60(5)
$Gd^{3+} + L \leftrightarrows GdL^{3+}$	5.43(3)
$Dy^{3+} + L \leftrightarrows DyL^{3+}$	5.54(7)
$Er^{3+} + L \leftrightarrows ErL^{3+}$	5.47(5)
$Lu^{3+} + L \leftrightarrows LuL^{3+}$	5.38(3)
$UO_2^{2+} + L \leftrightarrows UO_2L^{2+}$	5.78(5)

[a]Reference 11.

Table 5. Ideal M–N (N = pyridyl donor) and M–O (O from aqua ligand) Bond Lengths, Which Are the Average M–N and M–O Bond Lengths Obtained from the CSD[24] for Polypyridyl and Aqua Complexes of Ln(III) Ions[a,b,c]

metal ion	M–N[d] (pyridyl)	M–O[d] (aqua O)	ΣU(qpy complex) (kcal mol^{-1})	ΣU(DPP complex) (kcal mol^{-1})
La(III)	2.73(3)	2.56(6)	11.86	1.78
Ce(III)	2.70(3)	2.53(5)	11.52	1.56
Pr(III)	2.68(3)	2.51(5)	11.35	1.47
Nd(III)	2.66(4)	2.50(5)	11.13	1.33
Pm(III)	(2.64)[e]	(2.475)[e]	11.05	1.33
Sm(III)	2.62(5)	2.45(6)	11.14	1.50
Eu(III)	2.61(4)	2.44(7)	11.16	1.56
Gd(III)	2.60(4)	2.42(4)	11.32	1.76
Tb(III)	2.58(5)	2.41(5)	11.29	1.81
Dy(III)	2.56(3)	2.38(5)	11.63	3.24
Ho(III)	2.55(3)	2.37(5)	11.75	3.40
Er(III)	2.53(3)	2.36(5)	11.85	3.58
Tm(III)	2.52(3)	2.35(6)	12.02	3.79
Yb(III)	2.51(4)	2.33(6)	12.42	4.23
Lu(III)	2.51(3)	2.32(4)	12.64	4.44

[a]The ideal M–N and M–O lengths were used in MM calculations on Ln(III) complexes containing polypyridyl and aqua ligands. [b]Additional Ln–N for saturated N donors, and Ln-O for unidentate carboxylates, are available as Supporting Information. [c]The calculated[27] strain energies of the $[Ln(qpy)(H_2O)_5]^{3+}$ and $[Ln(DPP)(H_2O)_5]^{3+}$ complexes are given in kcal mol^{-1}. [d]Units are Å. [e]Bond lengths for Pm(III) estimated by interpolation between Nd(III) and Sm(III).

RESULTS AND DISCUSSION

Formation Constants. The approach[7,8] to studying the aqueous solution chemistry of ligands of low water solubility such as tpy and DPA, applied here to DPP, gives improved results. The omission of the background salt,[7,8] for example, 0.1 M $NaClO_4$, which salts the neutral ligand out, and use of a stock solution of DPP in MeOH, gives well solubilized solutions. This is evidenced

dx.doi.org/10.1021/ic3002509 | Inorg. Chem. 2013, 52, 15–27

by the absence of light scattering peaks (Figures 2a and 3), at 10^{-5} M DPP rather than only 4×10^{6} M DPP, as was achieved previously[1] by dissolving DPP in acidic solutions. The approach adopted here for the alkali earth M(II) ions and the Ln(III) ions, of titrating free 10^{-5} M DPP with a solution of the metal perchlorate, gives a very direct and straightforward determination of log K_1. The titrations with Ln(III) ions should be carried out close to pH 5.0 to avoid the presence of hydroxy species in solution. The formation constants obtained here for some Ln(III) ions are given in Table 4. These are somewhat lower than those obtained previously,[1] as would be expected where those determined previously[1] were at ionic strength (μ) 0.1 M, while those determined here are at $\mu = 0$ M.

In Figure 4 is shown the variation of log K_1 for DPP as a function of $1/r^+$ for the Ln(III) ions, where r^+ is the ionic radius[15]

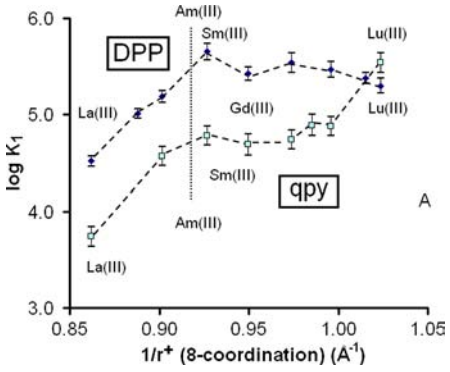

Figure 4. Variation of log K_1(DPP) and log K_1(qpy) (all at ionic strength = 0) for some Ln(III) ions as a function of the number $1/r^+$ (r^+ = ionic radius for eight-coordination[13]) in the Ln(III) ion. The value of $1/r^+$ for Am(III) is indicated on the diagram to show how close it is to Sm(III), which appears to be an optimal size for forming stable complexes with DPP or qpy. Formation constant data for DPP this work and reference 1, log K_1 values for qpy reference 12 in 50% methanol. Error bars indicate the standard deviations for the log K_1 values.

of the eight-coordinate ions. The eight-coordinate radii were used as an indication of relative metal ion size, rather than possibly more realistic nine-coordinate radii, so as to include Am(III), for which only an eight-coordinate radius is given.[15] Also included in Figure 4 are log K_1 values for the less preorganized DPP analogue qpy.[14] The qpy log K_1 values were determined[14] in 50% MeOH/H_2O because of the surprising fact that qpy is less soluble in aqueous solution than the bulkier DPP. Comparison of log K_1 values for Ln(III) ions with polypyridyl ligands such as tpy determined in aqueous solution[8] with those determined[40] in 50% MeOH/H_2O suggests that the difference in log K_1 values determined in these two solvents is quite small, so that comparisons such as those in Figure 4 can be made, bearing in mind that differences might also be at least partly due to the different solvents.

Figure 4 shows that there is a peak in log K_1 for both DPP and qpy at Sm(III), which is also observed for other polypyridyl ligands such as tpy,[41] MPP,[11] and DPA.[41] To understand the special position of Sm(III) in diagrams such as Figure 4, the strain energies of the $[Ln(qpy)(H_2O)_5]^{3+}$ and $[Ln(DPP)(H_2O)_5]^{3+}$ complexes were calculated for Ln(III) = La(III) through Lu(III) using the program HyperChem.[33] The average M−N (N = pyridyl donor) and M−O (O = aqua ligand) obtained from the CSD[24] (Table 5) were used in the MM calculations as ideal bond lengths. The values of the total strain energy (ΣU) for the $[Ln(qpy)(H_2O)_5]^{3+}$ and $[Ln(DPP)(H_2O)_5]^{3+}$ complexes are given in Table 5. In Figure 5 is shown the variation of ΣU as a function of decreasing M−N length for the

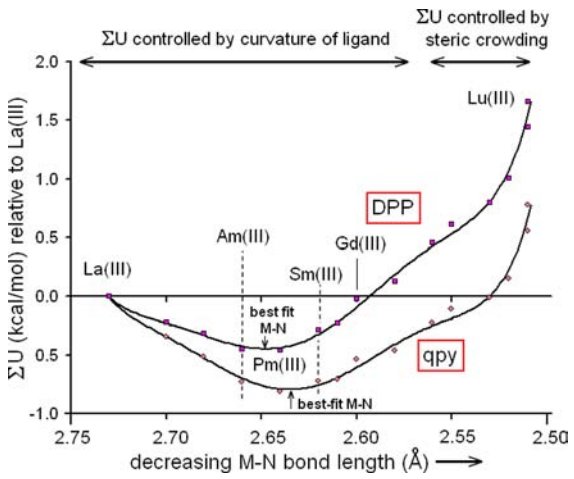

Figure 5. Strain energy (ΣU) for $[Ln(qpy)(H_2O)_5]^{3+}$ and $[Ln(DPP)(H_2O)_5]^{3+}$ complexes relative to the Ln(III) = La(III) complex, calculated by MM (molecular mechanics) as a function of M−N bond length. The calculations were carried out using the MM+ force field present in HyperChem[20] with ideal M−N and M−O bond lengths (Table 5) obtained from the CSD.[17] The M−N bond lengths are plotted in decreasing order to facilitate comparison with Figure 4. The solid lines are two sixth-order polynomials fitted to the calculated values of ΣU versus M−N length to facilitate calculation of the best-fit M−N lengths, and to aid in visualizing the relationships between U and M−N length. The curves otherwise have no physical significance.

$[Ln(qpy)(H_2O)_5]^{3+}$ and $[Ln(DPP)(H_2O)_5]^{3+}$ complexes. The curves fitted to the calculated values of ΣU as a function of M−N length in Figure 5 were generated from sixth order polynomials, and were used to aid in determining the best-fit M−N lengths for the $[Ln(qpy)(H_2O)_5]^{3+}$ and $[Ln(DPP)(H_2O)_5]^{3+}$ complexes as the M−N lengths corresponding to the minimum values of ΣU. One should emphasize that the polynomials do not represent any physical model, and as such were used only to aid in visualization of the fairly complex curves, as well as in indicating the energy minima of the curves. One sees that Sm(III) with a strain-free MN length with pyridyl donor ligands of 2.62 Å, lies quite close to the best-fit sizes for coordination with qpy or DPP of 2.636 Å and 2.647 Å, respectively. The Ln(III) ion that appears to fit qpy and DPP best is the Pm(III) cation, noting that the radioactive Pm does not occur in nature. However, Figure 5 indicates that the special position of Sm(III) in Figure 4 is because it fits qpy and DPP the best of the Ln(III) ions studied. The observed stability of Ln(III) ions with ligands may be understood as a balance between steadily increasing M−L (L = ligand) bond strengths in passing from La(III) to Lu(III), modified by steric strain effects. Thus, one sees a strong increase in log K_1 in passing from La(III) to Sm(III), which would involve both increasing M−L bond strengths and decreasing ΣU. For Ln(III) ions smaller than Sm(III), there would now be an increase in ΣU offsetting the increasing M−L bond strengths, with a decrease in log K_1.

The factors governing ΣU values of the $[Ln(qpy)(H_2O)_5]^{3+}$ and $Ln(DPP)(H_2O)_5]^{3+}$ complexes appear to be quite complex based on the appearance of the ΣU vs M−N length curve in Figure 5. The minima in ΣU at around an M−N length of 2.64 Å for these complexes appear to be governed by at least two factors. From La(III) through Sm(III), ΣU decreases because the repulsive van der Waals forces between the nonbonded H atoms

dx.doi.org/10.1021/ic3002509 | Inorg. Chem. 2013, 52, 15−27

at the 3-positions of the pyridyl groups decrease with decreasing metal ion size. In Figure 6 is shown the MM generated structure

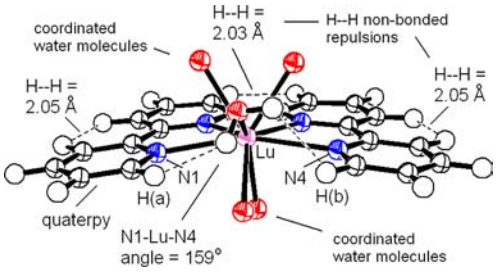

Figure 6. MM generated structure of $[Lu(qpy)(H_2O)_5]^{3+}$. Hydrogen atoms on the coordinated water molecules have been omitted for clarity, except for one water in the foreground. The close approach is shown of about 2.16 Å of the H-atoms on this water to the H-atoms labeled H(a) and H(b) on the qpy ligand. There are many such short nonbonded distances, too numerous to show here, between the O and H atoms of the coordinated water molecules, and the H, C, and N atoms of the qpy ligand. The structure shows the close approach of the H atoms at the 3 and 5 positions of adjacent pyridyl groups, giving HH nonbonded separations in the vicinity of 2.0 Å indicated on the drawing. The structure also shows the bowing of the qpy ligand, which results in N1−Ln−N4 angles smaller than the ideal angle of 180° for planar qpy, which destabilizes complexes of Ln(III) ions increasingly at M−N lengths shorter than those for Sm(III). Drawing made with ORTEP.[31]

of $[Lu(qpy)(H_2O)_5]^{3+}$, showing the H--H separations between the H atoms at the 3-positions on the coordinated qpy. These are quite short at about 2.00 to 2.05 Å in the Ln(III)/qpy and Ln(III)/DPP complexes, which is well short of the sum of the van der Waals radii of two nonbonded H atoms of 2.40 Å, which should be a cause of considerable steric strain. As the metal ion gets smaller, the curvature of the qpy or DPP ligand increases, and the H--H separations increase slightly, leading to some decrease in ΣU. After the minimum in ΣU at around Sm(III), the decreasing size of the metal ion causes increasing bowing of the qpy or DPP ligand, resulting in increasing ΣU. One sees this in Figure 6, where the N1−Lu−N4 angle is 159.0°, instead of an angle in planar qpy of 180° with M−N lengths of 2.82 Å. This same bowing, as generated by MM here, is seen in the only comparable structure,[26] for the small Y(III) coordinated with qpy, where the average Y−N distance is 2.466 Å, and the N1−Y−N4 angle is 154.7°. It appears from Figure 5 that at M−N lengths of about 2.55 Å the rate of rise in ΣU begins to flatten off, only to rise more steeply again at shorter M−N lengths approaching 2.50 Å. The interpretation of this is that the effect of decreasing bond length on the extent of bowing and hence the ΣU of qpy or DPP begins to flatten off with decreasing M−N bond length, but ΣU then begins to rise again because of steric crowding effects. The effects of steric crowding can be seen in the paper of Semenova and White[25] on the structures of Ln(III) ion complexes with tpy ligand and the balance of the coordination sphere occupied by aqua ligands. For La(III) and Er(III), there are six coordinated water molecules, giving a total coordination number (C.N.) of nine. For the smaller Tm(III), Yb(III), and Lu(III) ions, the C.N. drops to eight, with only five coordinated water molecules. One notes that it is in the region of M−N lengths of the four smaller Ln(III)/qpy complexes from Er(III) to Lu(III) in Figure 5 that steric crowding effects are predicted by the MM calculations to become progressively energetically more unfavorable, and it is in this region of M−N length for Ln(III)/tpy complexes that the transition from 9-coordinate (Er(III)) to 8-coordinate (Tm(III) to Lu(III)) occurs.[25]

The indications from the MM calculations that relate to the variation of log K_1 with size of Ln(III) ion in Figure 4 are that the peak in log K_1 that occurs at Sm(III) for DPP, qpy,[14] and also other polypyridyl ligands,[41] is controlled by (1) H--H non-bonded separations of much less than the sum of the van der Waals radii of[42] 2.40 Å, which distances become shorter as M−N bond length increases for the Ln(III) ion, and so destabilize DPP and qpy complexes of larger Ln(III) ions, and (2) for Ln(III) ion smaller than Sm(III), the DPP or qpy ligand becomes increasingly more bowed to accommodate the too-short M−N lengths, with the resulting increasing ΣU destabilizing the complexes, and (3) for the smallest Ln(III) ions Er(III) through Lu(III), steric crowding resulting largely from close contacts between the coordinated water molecules and the DPP or qpy ligands, ΣU rises more rapidly and destabilizes the complexes of these smallest Ln(III) ions. An important aspect of Figure 4 is that log K_1 for the qpy complexes appears to continue to rise strongly for the smaller Ln(III) ions, and the qpy complexes appear to become more stable than the DPP complexes for Lu(III). This is point (4) that can be gleaned from Figure 5, which is that ΣU rises more rapidly with increasing M−N length from La(III) to Lu(III), and eventually destabilizes the complexes of DPP to the point where their stability falls below that of the qpy complexes for the smallest metal ions. One would suggest that this effect relates to the greater rigidity of the DPP ligand, which is thus less able to accommodate too-small metal ions than is the qpy ligand.

To compare the selectivity patterns of polypyridyl ligands across the Ln(III) series with ligands of other types, in Figure 7 is shown the increase in log K_1 for the Ln(III) series[13] relative to Ln = La for a variety of ligands, plotted as a function of $1/r^+$ (r^+ = ionic radius for 8-coordination). One sees that more flexible ligands such as IDA and EDTA that are built from saturated organic groups show a fairly regular increase in log K_1 across the series of Ln(III) ions with decreasing ionic radius, with no strong local maximum at Sm(III). The larger DTPA ligand, of higher denticity than IDA or EDTA, appears to suffer steric difficulties for Ln(III) ions somewhat smaller than Gd(III), evidenced by a strong falloff in the rate of increase of log K_1 values, which is traditionally regarded as being due to steric crowding effects. The small DIPIC ligand forms two rigid five-membered chelate rings, and like a sterically similar polypyridyl ligand, displays a maximum in log K_1 at Sm(III). This is also true for acetate, which forms rigid 4-membered chelate rings with Ln(III) ions,[24] which also appears to cause steric difficulties beyond Ln(III) = Gd(III). One can summarize Figure 7 as showing that the rigid DPP ligand has a maximum in log K_1 at Sm(III), which is sterically the best-fit Ln(III) ion for polypyridyl ligands, which is also observed for the rigid DIPIC and acetate ligands. Flexible ligands such as IDA and EDTA show a steady increase in log K_1 with decreasing r^+, with little apparent in the way of steric problems. The larger DTPA ligand appears to cause steric problems beyond Ln(III) = Gd(III), with a marked drop-off in the rate of increase in log K_1, which is traditionally thought to be due to steric crowding effects.

Implications of Results on Ln(III) Ions for Separations from Am(III). An important facet of the work on Ln(III) ions reported here is how this can lead to an understanding of ligand-design factors that should be considered in developing improved polypyridyl-type extractants for Am(III). One result of considerable import from Figures 4 and 5 is that Am(III) is very close to being a

dx.doi.org/10.1021/ic3002509 | Inorg. Chem. 2013, 52, 15−27

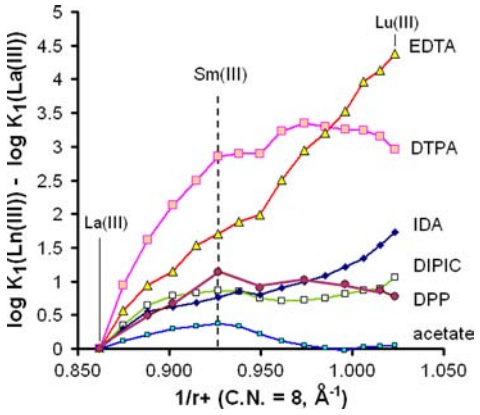

Figure 7. Variation of the increase in log K_1 for a selection of complexes of Ln(III) ions, relative to log K_1 for the corresponding La(III) complex, plotted as a function of $1/r^+$, where r^+ is the ionic radius for 8-coordination of the Ln(III) ions. Ionic radii from reference 13, log K_1 values from reference 11 and this work. Abbreviations: EDTA, erthylenediamine-*N*,*N*,*N*′,*N*′-tetraacetate; DTPA, diethylenetriamine-*N*,*N*,*N*′,*N*′,*N*″-pentaacetate; IDA, iminodiacetate; DIPIC, pyridine-2,6-dicarboxylate.

best-fit size for coordinating with ligands of the qpy or DPP type. The authors are currently collaborating with others in a study of the complexes of polypyridyl ligands of the qpy and DPP type to evaluate this conclusion. If Am(III) is indeed a best-fit cation for coordinating with qpy and DPP, this would explain the good selectivity for Am(III) relative to Ln(III) cations obtained[3] for extractants based on BTphen, which sterically should quite closely resemble DPP. No structure of an Am(III) complex coordinated to a pyridyl donor ligand is reported in the CSD. One notes that Ln−N bonds to saturated N-donors are on average 0.06 ± 0.01 Å longer than Ln−N bonds to pyridyl N-donors, so that, for the single reported structure of Am(III) with saturated N-donors,[43] where Am−N averages 2.72 Å, one estimates an Am−N length for pyridyl donors of 2.66 Å. This Am−N bond length is (Figure 5) the best-fit length for coordination, which would explain the good selectivity for Am(III) relative to Ln(III) cations obtained[3] for extractants based on BTphen, which sterically should quite closely resemble DPP. The MM calculations suggest that ΣU for the DPP complexes should be some 0.5 kcal mol^{-1} higher for the smaller Gd(III) (a prime target in the separations because of its high neutron capture cross-section) than for Am(III), which would translate into a contribution to the Am(III)/Gd(III) selectivity of a factor of 2.3 times more selective. As far as design strategies go, further rigidification of tetrapyridyl type ligands may produce even better Am(III)/Gd(III) selectivity.

Complexes Formed by UO_2^{2+} with DPP in Aqueous Solution. The UO_2^{2+} cation is more acidic than the Ln(III) ions, with a log $K_1(OH^-)$ value[13] of 7.6 for UO_2^{2+}, compared to log $K_1(OH^-)$ ranging for Ln(III) ions from 4.7 for La(III), up to log $K_1(OH^-)$ = 5.8 for Lu(III) (all at μ=0.5 M). This means that the complexes of UO_2^{2+} with ligands with N donor groups only are rather susceptible to hydrolysis, as seen for the predicted[9,44] log $K_1(NH_3)$ value for UO_2^{2+} (eq 1):

$$UO_2(NH_3)^{2+} + H_2O \leftrightarrows UO_2(OH)^+ + NH_4^+ \quad (1)$$

With log $K_1(NH_3)$ predicted[44] for UO_2^{2+} as 2.0, pK_w as 13.78,[13] log $K_1(OH^-)$ for UO_2^{2+} as 7.7,[13] and p$K_a(NH_3)$ as 9.26[13] (all at μ = 0.1 M), one calculates the equilibrium coefficient (Q) for eq 1 as $10^{1.2}$. The latter value of Q suggests that the UO_2^{2+}/NH_3 complex would not be able to exist in appreciable quantities in aqueous solution at any pH (eq 1 is pH independent). However, the DPP ligand has the advantage of being a tetradentate chelate of higher preorganization,[9,10] which should lead to a considerably higher log K_1 than predicted for the NH_3 complex. DPP, and also other polypyridyl ligands, have a much lower pK_1 than do ligands with saturated N donors such as NH_3, which should make Q much smaller for equations involving DPP that are analogous to eq 1.

In Figure 8 is shown a set of spectra of a 1:1 UO_2^{2+}/DPP 10^{-5} M solution in the pH range 2.7 to 5.38. There are no large light scattering peaks near 200 nm suggesting the formation of precipitates, and as the pH is raised, a sharp peak appears at 285 nm, typical of the presence of a metal ion complexed with DPP, as seen for Ca(II) and Pr(III) in Figures 2a and 3. Analysis of the spectra yields log K_1(DPP) for UO_2^{2+} = 5.78(5), which is the first example of a formation constant[13] of the UO_2^{2+} cation with a purely neutral N donor ligand in aqueous solution. Examination of Table 4 shows that the UO_2^{2+} cation has somewhat higher affinity for DPP than do the Ln(III) cations. This is consistent with attempts to estimate the affinity of hydrolysis-prone cations for N donor ligands,[13,21−23,44] which suggest that the UO_2^{2+} cation should have a somewhat higher affinity for such ligands than do the Ln(III) cations. One would expect the UO_2^{2+} cation to form complexes of reasonable stability with a ligand such as DPP from the steric point of view, as UN bonds involving pyridyl N donors found in the CSD[24] average 2.59 ± 0.04 Å (171 structures), not too far from the best-fit MN length of 2.647 Å in Figure 5.

Affinities of Alkaline Earth Cations for DPP. The log K_1(DPP) values (Table 4) for the alkaline earth cations show the order commonly found for these cations with ligands of denticity three or higher, of Mg(II) < Ca(II) > Sr(II) > Ba(II). The lower log K_1 for Mg(II) than Ca(II) with most ligands of higher denticity relates to the common presence of five-membered chelate rings, which favors the larger metal ion.[9] The effect of chelate ring size on metal ion selectivity becomes enhanced with higher denticity, and so with ligands of lower denticity one finds the order of log K_1 of Mg(II) > Ca(II). This is seen for a selection of polypyridyl ligands in Scheme 3:

The variation in M−N bond length for pyridyl N donors along the series of alkali-earth metal ions as indicated by average M−N lengths in the CSD[24] is as follows: Mg(II), 2.21 ± 0.08 Å (171 structures); Ca(II), 2.57 ± 0.04 Å (81 structures); Sr(II), 2.73 ± 0.07 Å (44 structures); Ba(II), 2.93 ± 0.06 Å (105 structures). Mg(II) appears to be too small for the five-membered chelate ring (Scheme 2), while Sr(II) and Ba(II) are too large. Ca(II) belongs to a special group of metal ions, which includes La(III) and Th(IV), that have an octahedral ionic radius close to 1.0 Å, which corresponds to having best-fit M−L lengths most suited to five-membered chelate rings formed by pyridyl donors, saturated N donors such as are present in polyamines such as ethylenediamine, and carboxylates, such as are present in ligands such as oxalate, or in polyaminocarboxylates such as EDTA.

Structure of $[Zn(DPP)_2](ClO_4)_2$ (1). The structure of the complex cation $[Zn(DPP)_2]^{2+}$ is seen in Figure 9. The Zn(II) is 6-coordinate, with one pyridyl group from each DPP left noncoordinated, and placed above the central benzo group from the other DPP ligand. The average separation between the atoms forming the rings of the noncoordinated pyridyl groups and the best-fit planes of the central benzo groups is about 3.4 Å, which would possibly be appropriate[45] for a π-stacking interaction, except that the planes formed by noncoordinated pyridyl group and the central benzo group of the second DPP are not exactly parallel, so that this may represent a weak π-stacking interaction.

dx.doi.org/10.1021/ic3002509 | *Inorg. Chem.* 2013, 52, 15−27

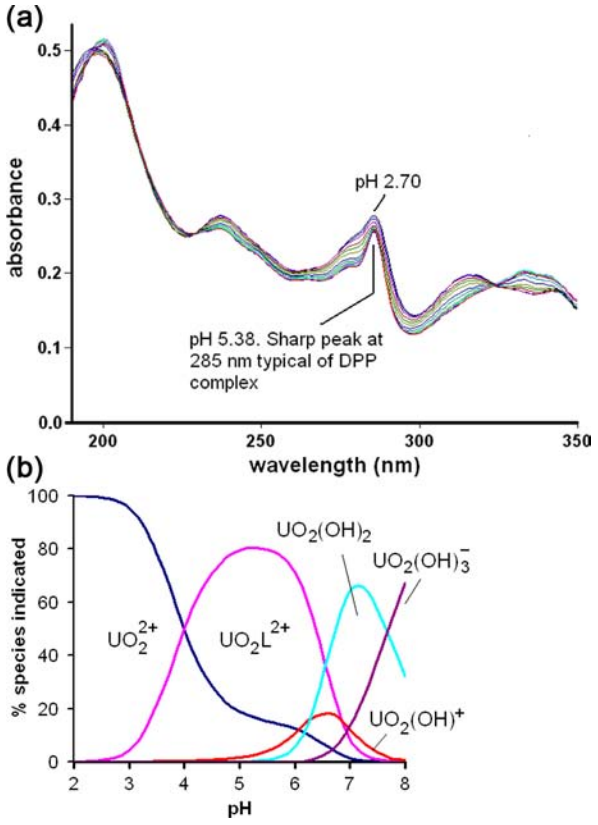

Figure 8. (a) Spectra of 10^{-5} M DPP plus 10^{-5} M UO_2^{2+} from pH 2.70 to 5.38, 25 °C, $\mu = 0$. The spectra can be analyzed to yield log K_1(DPP) = 5.77 for the UO_2^{2+} cation. (b) Species distribution diagram for 10^{-5} M DPP ('L' = DPP on the diagram) plus 10^{-58} M UO_2^{2+}, calculated using log K_1(DPP) = 5.78 determined here for the UO_2^{2+}/DPP complex, plus protonation constants for DPP (Table 4) and literature values[11] for hydroxide complexes of the UO_2^{2+} cation. Diagram calculated using the Excel program.[26]

Scheme 3. Effect of Increasing Denticity on log K_1 Values for Mg(II) and Ca(II) with Some Polypyridyl Ligands[a]

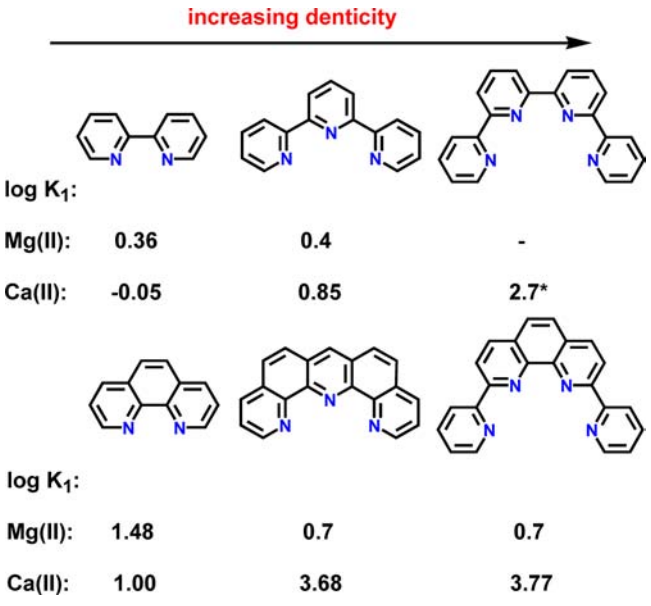

[a]Log K_1 values are from this work, and references 7, 8, 11, and 14. *50% MeOH.

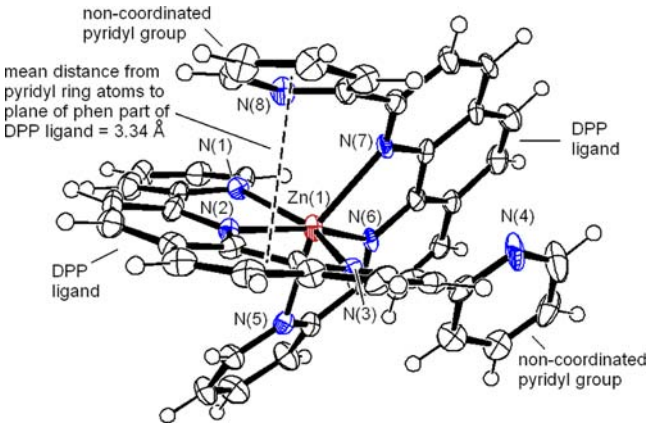

Figure 9. Structure of one $[Zn(DPP)_2]^{2+}$ complex cation from (**1**), showing the numbering scheme for the donor atoms of DPP. Thermal ellipsoids drawn at 50% confidence level, drawing made with ORTEP.[31]

The structure of $[Zn(DPP)_2]^{2+}$ is quite similar to that of $[Zn(qpy)_2]^{2+}$, which also has[46] a six-coordinate Zn(II) with one pyridyl group from each qpy being noncoordinated, and laid over the adjacent qpy ligand, but possibly not sufficiently well aligned to be involved in strong π-stacking. Similar structures were also observed[46] for $[Ni(qpy)_2]^{2+}$ and $[Fe(qpy)_2]^{2+}$. The structures of the complexes of these small ($r^+ < 0.8$ Å) metal ions with DPP or qpy show they are unable to raise their C.N.'s above 6 to coordinate with these polypyridyl ligands. Where a single qpy is coordinated to Zn(II), as in $[Zn(qpy)(H_2O)_2]^{2+}$, all four N donors of the ligand are coordinated to the Zn(II), but there is apparently considerable steric strain, as evidenced by, for example, a N−Zn−N angle involving the two terminal pyridyl groups of the qpy of 135.9°, as opposed to an angle of 90° expected for a regular octahedron.[46]

Structure of $[Bi(DPP)(H_2O)_2(ClO_4)_2]ClO_4$ (2). The structure of the complex cation in **2** is seen in Figure 10. The Bi is eight coordinate, with the coordination sphere comprising the four donors from the DPP, two water molecules, and two unidentate perchlorates. As is so often found for Bi(III),[47−49] and also Pb(II),[50−53] there appears to be a stereochemically active lone pair, which is situated opposite the most covalently bound donor atoms, in this case the N donors of the DPP. The indications of a stereochemically active lone pair are as follows:[50] (1) short M−L bonds on the side of the metal ion away from the proposed site of the lone pair, that usually involve the most covalently bound donor atoms present,[52] (2) M−L bonds that become progressively longer as one moves toward the proposed site of the lone pair, and (3) an apparent gap in the coordination geometry at the proposed site of the lone pair, although there may be a very long M−L bond at this site, usually more than 3.2 Å for oxygen donors that usually occupy such a site as the least covalently bound donor atoms present. In agreement with these 3 requirements, the Bi−N bond lengths to the two central N donors of the DPP in **1** are the shortest of the BiN lengths, averaging 2.412 Å, in line with the suggestion (Figure 10) that the lone pair is situated opposite these two N donors. The Bi−N lengths to the two outer N donors of the DPP are somewhat longer at 2.526 Å, being closer to the position of the lone pair. The two water molecules are slightly closer to the lone pair than the two outer N donors of the DPP, with Bi−O bond lengths averaging 2.360 Å, which are somewhat shorter than the Bi−N lengths because the covalent radius of O is 0.05 Å smaller than

dx.doi.org/10.1021/ic3002509 | Inorg. Chem. 2013, 52, 15−27

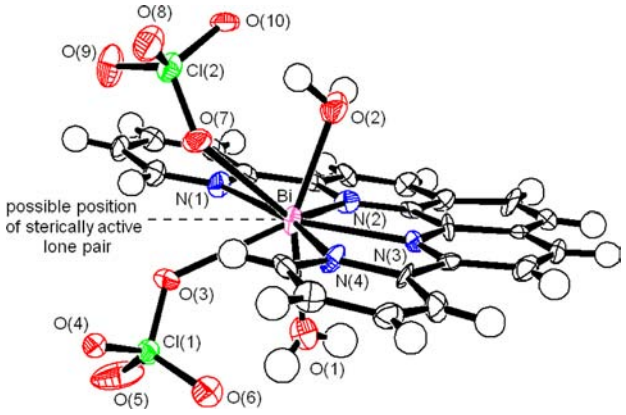

Figure 10. Structure of one $[Bi(DPP)(H_2O)_2(ClO_4)_2]^+$ complex cation from (**2**), showing the numbering scheme for the donor atoms of DPP and other ligands coordinated to the Bi atom. The proposed position of the stereochemically active lone pair is discussed in the text. Thermal ellipsoids drawn at 50% confidence level, drawing made with ORTEP.[31]

that of N.[54] The Bi−O lengths to the two perchlorates average 2.76 Å, being closest to the proposed position of the lone pair in Figure 10.

The structure of the $[Bi(DPP)(H_2O)_2(ClO_4)_2]^+$ cation is of some interest in that Bi^{3+} is a large cation, with an ionic radius for six-coordination[15] of 1.03 Å, the same as for La^{3+}. The qpy ligand adapts to the too-small Ln(III) ions by folding along an axis running through the center of the ligand, as seen in Figure 6. This is not possible for the DPP complexes, with the rigid benzo group occupying this position, and so the DPP ligand adopts a slightly saddle-shaped structure to bring the N donor atoms of the ligand closer to the metal ion. This type of structure is observed in both the Bi(III)/DPP complex seen in Figure 10, and is also observed in the structures of the Ln(III)/DPP complexes generated by MM calculation, supporting the idea that the MM structures are accurate models of the Ln(III)/DPP complexes.

DFT Calculations on Ln(III) polypyridyl complexes. In lieu of structures of Ln(III) complexes of qpy, and DPP, which would clearly be helpful in understanding the selectivity patterns of these cations with polypyridyl ligands, DFT calculations were performed on some of the Ln(III) complexes. The structures of the tpy complexes of La(III) and Lu(III) were generated so as to evaluate the structural accuracy of the DFT calculations by comparison with reported solid state structures,[25] and to evaluate the role of steric crowding in destabilizing the complexes of polypyridyl ligands with the smaller Ln(III) cations. A selection of structural parameters for the La(III) and Lu(III) complexes of tpy, calculated by DFT, and observed,[25] are given in Table 6, and the structure of $[Lu(tpy)(H_2O)_5]^{3+}$ is shown in Figure 11. The average Ln−O bond lengths are predicted to be too long by about 0.07 Å, and the N−C−C−N torsion angles (χ) are predicted to be too small by about 3.9°, but otherwise the accuracy of prediction is impressive. In the case of χ(N−C−C−N) the DFT calculations correctly predict that these will be substantially larger for La(III) (11.4°) than Lu(III) (5.7°). It has been previously pointed out[10] that χ(NCCN) will increase with increase in metal ion size: χ(NCC−N) in bpy complexes is 27.6° with the very large Ba(II), with M−N bond lengths of 2.93 Å.[55]

The suggestion that the C.N. of the $[Ln(tpy)(H_2O)_n]^{3+}$ complexes drops from 9 (n = 6) to 8 (n = 5) in passing from La(III) to Lu(III) because of steric crowding with the smaller Lu(III) metal ion is supported by both the crystal structures[25] and the DFT calculations reported here. The structures of 8-coordinate $[Ln(tpy)(H_2O)_5]^{3+}$ and 9-coordinate $[Ln(tpy)(H_2O)_6]^{3+}$ as generated by DFT are shown in Figure 11. The sum of O--O nonbonded radii for two O atoms is 3.04 Å,[42] so that O--O nonbonded separations significantly shorter than this should be destabilizing. In Table 6 are shown the average O--O nonbonded separations for the oxygen atoms of adjacent coordinated water molecules in the Ln(III)/tpy complexes under consideration. For 9-coordinate $[Ln(tpy)(H_2O)_6]^{3+}$ complexes there are 9 fairly short O--O nonbonded distances. For the $[La(tpy)(H_2O)_6]^{3+}$ complex, the crystal structure shows[25] this average O--O nonbonded distance

Table 6. Selection of Structural Parameters for $[La(tpy)(H_2O)_6]^{3+}$ and $[Lu(tpy)(H_2O)_5]^{3+}$, Calculated Here by DFT, and Observed,[25] As Well As the Structure of $[Lu(tpy)(H_2O)_6]^{3+}$, Which Has Not Been Observed Experimentally

	$[La(tpy)(H_2O)_6]^{3+}$		$[Lu(tpy)(H_2O)_5]^{3+}$		$[Lu(tpy)(H_2O)_6]^{3+}$
	calc.	obsd.	calc.	obsd.	calc.
		Bond Length (Å)[a]			
M−N(1)	2.671	2.670	2.496	2.444	2.506
M−N(2)	2.711	2.684	2.464	2.396	2.501
M−N(3)	2.670	2.655	2.453	2.426	2.510
M−O (average)	2.62(3)	2.54(4)	2.36(1)	2.32 (3)	2.42(6)
		Bond Angle (deg)[a]			
N1−M−N2	61.8	62.1	66.6	66.6	65.7
N2−M−N3	61.8	61.3	66.6	67.9	65.6
		Torsion Angle (deg)[b]			
χ(N−C−C−N) (average):	11.4	15.6	5.7	8.3	8.6
		Non-bonded (Å)			
O--O (H_2O):[c] (average)	3.03(22)	3.02(26)	2.82(10)	2.86(13)	2.79(17)
H--H (pyridines):[d] (average)	2.00(2)	2.07(1)	2.01(1)	2.18(1)	2.01(1)

[a]The M−N bond lengths are to the pyridyl nitrogens. The N1 and N3 atoms are from the outer pyridyl groups, while N2 is from the central pyridyl group of tpy. The M−O average lengths are the average of the Ln−O lengths of the coordinated waters in each structure. [b]The χ(N−C−C−N) angles refer to atoms in the clefts of the tpy ligand. [c]The O--O nonbonded distances refer to the distances between O atoms from adjacent water molecules coordinated to the Ln(III) ion. There are 9 such distances for the 9-coordinate metal ions, and 6 for the 8-coordinate complexes. The number in parentheses indicates the range up or down of the O--O distance in the last two digits. [d]This is the average of the two H--H nonbonded distances between the H atoms at the 3 and 3′, or 5′ and 3″ positions on tpy for each structure. The number in parentheses indicates the range up or down of the O--O distance in the last digit.

dx.doi.org/10.1021/ic3002509 | Inorg. Chem. 2013, 52, 15−27

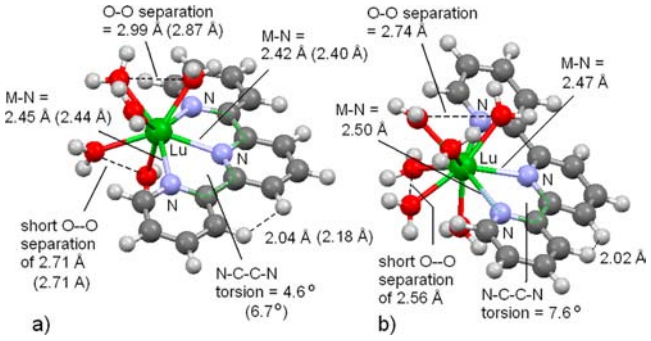

Figure 11. Structures of (a) 8-coordinate $[Lu(tpy)(H_2O)_5]^{3+}$ and (b) 9-coordinate $[Lu(tpy)(H_2O)_6]^{3+}$, generated by DFT as described in the text. Some bond lengths, nonbonded distances, and torsion angles of interest in (a) have crystallographic values indicated in parentheses.[25] The structures show the effect of greater steric crowding in (b) than (a), namely, (1) some of the many O--O nonbonded contacts shorter than the sum of the van der Waals radii[42] of 3.04 Å for two nonbonded O atoms, and (2) the lengthened Lu−N bonds in the 9-coordinate complex at (b) as compared with the 8-coordinate complex at (a). Drawing made with Mercury, part of the CSD suite of programs.[24]

to be 3.03 Å, while the DFT calculations suggest it to be 3.02 Å, only slightly shorter than the sum of the van der Waals radii. For the $[Lu(tpy)(H_2O)_6]^{3+}$ complex, for which no experimental structure is available,[24] the DFT calculations suggest that the same nine OO nonbonded distances average 2.79 Å, significantly shorter than the sum of the van der Waals radii of 3.04 Å, supporting the idea that steric crowding plays a part in reducing the C.N. of the complex of the smaller Lu(III) ion to 8, as observed[25] in the $[Lu(tpy)(H_2O)_5]^{3+}$ complex. Interestingly, in the latter complex, the OO nonbonded separations are still quite short, averaging 2.86 Å, but one must assume that the 9-coordinate $[Lu(tpy)(H_2O)_6]^{3+}$ is destabilized relative to the 8-coordinate $[Lu(tpy)(H_2O)_5]^{3+}$ because there are 9 short O--O nonbonded contacts in the 9-coordinate complex compared to 6 short contacts in the 8-coordinate complex.

Some structural parameters for the $[Ln(DPP)(H_2O)_5]^{3+}$ complexes generated by DFT and MM calculation here are shown in Table 7. The agreement between the two methods of structural prediction is reassuring. Again, the entirely empirical MM approach predicts shorter Ln−O bonds than DFT, which are likely to be more accurate. The average O--O nonbonded distances in the structures of the $[Ln(DPP)(H_2O)_5]^{3+}$ complexes generated by both MM and DFT show a steady decrease from being somewhat less than the sum of the van der Waals radii of two O atoms (3.04 Å) for the complex of the large La(III) complex (2.91 Å from DFT), to being significantly less for Lu(III) (2.67 Å). This supports the idea that the decrease in

Table 7. Selection of Structural Parameters for $[Ln(DPP)(H_2O)_5]^{3+}$ Complexes, (Ln = La, Sm, Gd, Er, and Lu) Calculated Here by DFT and by MM Calculation

	$[La(DPP)(H_2O)_5]^{3+}$		$[Sm(DPP)(H_2O)_5]^{3+}$		$[Gd(DPP)(H_2O)_5]^{3+}$	
	DFT	MM	DFT	MM	DFT	MM
			Bond Length (Å)[a]			
M−N(average outer):	2.706	2.691	2.610	2.602	2.593	2.573
M−N(average inner):	2.682	2.712	2.584	2.612	2.559	2.594
M−O (average):	2.62(3)	2.58(1)	2.52(4)	2.48(2)	2.49(2)	2.46(2)
			Bond Angle (deg)[a]			
N−M−N (outer two):	61.3	60.8	67.4	66.6	63.6	63.4
N−M−N (inner):	62.5	62.2	67.3	67.9	64.8	64.1
			Torsion Angle (deg)[b]			
χ(N−C−C−N) (average):	4.3(1)	0.5(4)	2.6(2)	0.9(1)	6.1(2.1)	0.9(1)
			Non-bonded (Å)			
O--O (H_2O):[c](average	2.91(15)	2.91(15)	2.78(13)	2.81(14)	2.75(13)	2.78(13)
H--H (pyridines):[d] (average)	1.97(13)	2.03(0)	2.00(2)	2.05(0)	2.00(1)	2.04(0)

	$[Er(DPP)(H_2O)_5]^{3+}$		$[Lu(DPP)(H_2O)_5]^{3+}$	
	DFT	MM	DFT	MM
		Bond Length (Å)[a]		
M−N(average outer):	2.547	2.536	2.533	2.507
M−N(average inner):	2.504	2.537	2.472	2.520
M−O (average):	2.47(6)	2.41(2)	2.42(2)	2.38(3)
		Bond Angle (deg)[a]		
N−M−N (outer two):	64.6	63.7	65.0	65.0
N−M−N (inner):	65.9	65.1	66.2	65.3
		Torsion Angle (deg)[b]		
χ(N−C−C−N): (average)	6.1(2.1)	0.9(1)	4.1(2.0)	1.1(0)
		Non-bonded (Å)		
O--O (H_2O):[c] (average)	2.70(13)	2.72(12)	2.67(08)	2.70(12)
H--H (pyridines):[d] (average)	2.03(3)	2.07(0)	2.02(2)	2.05(0)

[a]The M−N bond lengths are the average of those to the two outer and the average of those to the two inner pyridyl nitrogens, of DPP. The M−O average lengths are the average of the Ln-O lengths of the five coordinated waters in each structure. [b]χ(N−C−C−N) refers to the atoms in the two outer clefts of the DPP ligand (see Scheme 4). [c]The O--O nonbonded distances refer to the distances between O atoms from adjacent water molecules coordinated to the Ln(III) ion. There are 6 such distances in the $[Ln(DPP)(H_2O)_5]^{3+}$ complexes. The number in parentheses indicates the range up or down of the O--O distance in the last two digits. [d]This is the average of the two H--H nonbonded distances between the H atoms at the 3 and 3′, or 8 and 3″ positions on DPP for each structure (see Scheme 4). The number in parentheses indicates the range up or down of the O--O distance in the last digit.

dx.doi.org/10.1021/ic3002509 | Inorg. Chem. 2013, 52, 15−27

the rate of increase in log K_1 for DPP complexes as the size of the Ln(III) ion decreases from Er(III) to Lu(III) in Figure 5 is due to increasing steric crowding, possibly accompanied by a decrease in C.N. as observed[25] for the tpy complexes.

Figure 5 indicates a variation in U for $[Ln(DPP)(H_2O)_5]^{3+}$ complexes as a function of metal ion size, that has a minimum in U close to Ln = Sm. Both the MM and DFT calculations predict an Sm−N bond length close to 2.61 Å. One might expect to see the chelate ring geometry as being closest to an ideal value of 120° for angles a through f in Scheme 4. However, for all the

Scheme 4. Structural Parameters of Interest in $[Ln(DPP)(H_2O)_5]^{3+}$ Complexes for Ln = La, Sm, Gd, Eu, and Lu

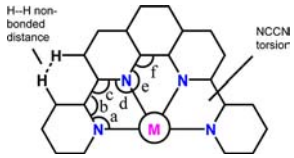

Ln(III) ions, these angles are fairly close to 120°, and what appears to vary is the χ(N−C−C−N) angle shown in Scheme 4. As seen in Table 7, χ(N−C−C−N) angles are La(III), 4.3; Sm(III), 2.6; Gd(III), 6.1; Eu(III), 6.1; Lu(III), 4.1. The metal ions away from Sm(III) in size appear to achieve better chelate ring geometry with DPP by altering the χ(N−C−C−N) angle, and it is probably the distortion of χ that contributes to the destabilization of the complexes of Ln(III) ions of a size different from Sm(III). There are probably many other small steric effects that contribute to the position of the minimum in U at Sm(III) in Figure 5. The differences in U between the DPP complexes of different Ln(III) ions in Figure 5 are in any case small, and so there should not be large obvious steric effects that can be identified as causes of the position of the minimum in U.

It has been assumed in this work that the complexes of DPP and qpy will be 9-coordinate for the larger Ln(III) ions, with five coordinated water molecules. This appears reasonable because the structure of the tpy complexes of the larger Ln(III) ions shows them to be 9-coordinate, with six coordinated water molecules.[25] Examination of the CSD[24] shows that for the larger Ln(III) ions, the most common C.N. is 9. It was also assumed that the complexes of the smaller Ln(III) complexes of DPP and qpy would be 9-coordinate, when in fact it is more likely that they are 8-coordinate, which is the case for the $[Ln(tpy)(H_2O_5)]^{3+}$ complexes.[25] This was because for MM one cannot compare the strain energies of molecules with differing numbers of atoms. One instead observes in Figure 5 an upward increase in U as the size of the Ln(III) ions beyond Er(III) decreases, which is itself suggestive of what the factors might be that control C.N.

CONCLUSIONS

The work reported here shows the following: (1) A peak in log K_1 for DPP complexes with Ln(III) ions occurs at Sm(III), which has an average[24] M−N bond length of 2.62 Å, (2) the latter bond length is suggested by MM calculations to be close to the best-fit MN length for $[Ln(DPP)(H_2O)_5]^{3+}$ complexes of 2.65 Å, (3) MM calculations on qpy and DPP complexes, and also on tpy and DPA complexes,[7] indicate that a preference for metal ions with M−N lengths close to 2.65 Å will occur for all polypyridyl-type ligands, including possibly also those containing triazine groups, (4) the MM calculations suggest that the variation of strain energy (ΣU) for $[Ln(DPP)(H_2O)_5]^{3+}$ complexes is controlled by the curvature of the DPP ligand at longer M−N lengths, but that for the Ln(III) ions smaller than Er(III), ΣU is controlled by steric crowding, (5) Am(III) appears[24] to have MN lengths close to those of Sm(III), so that an important aspect of the selectivity of polypyridyl type ligands for Am(III) compared to the smaller Gd(III) ion may be found in the future to depend on the above metal ion size-based selectivity, (6) solvent extractants based on polypyridyl type ligands, incorporating also triazine groups, for the separation of Am(III) and Ln(III) ions in the treatment of nuclear waste, should have a component of size-based selectivity dependent on the good fit of Am(III) with polypyridyl type ligands such as DPP, (7) the selectivity pattern of DPP with the alkali-earth metal ions shows a similar preference for Ca(II), which has[24] the most appropriate M−N lengths. The lower stability of the Mg(II) complexes than the Ca(II) complexes of most ligands of denticity higher than two, or in some cases three, is dependent on the small size of Mg(II) and its poor fit[14] with the five-membered chelate rings most commonly present in such ligands. (8) The low pK_a of 4.41 of DPP promotes resistance to hydrolysis of its complexes with acidic metal ions in aqueous solution. The high log K_1 values of DPP with metal ions with M−N lengths close to 2.65 Å, makes DPP a good candidate for the first example[11] of a log K_1 value for the acidic UO_2^{2+} cation in aqueous solution with a ligand containing N donor groups only. A value of log K_1 = 5.78 is reported for the UO_2^{2+} cation, consistent with its average[24] U−N length of 2.59 Å, reasonably close to the best-fit size for DPP of 2.65 Å.

ASSOCIATED CONTENT

Supporting Information

Average Ln_-N bond lengths in Ln(III) complexes of 1,10-phenanthroline and Ln−O bond lengths in carboxylate and aqua complexes of Ln(III) cations. This material is available free of charge via the Internet at http://pubs.acs.org.

AUTHOR INFORMATION

Corresponding Author

*E-mail: thummel@uh.edu (R.P.T.), hancockr@uncw.edu (R.D.H.).

Notes

The authors declare no competing financial interest.

ACKNOWLEDGMENTS

The authors A.N.C., G.M.C., N.J.W., H.L., and R.D.H. thank the University of North Carolina Wilmington and the Department of Energy (Grant # DE-FG07-07ID14896) for generous support for this work. R.P.T. and G.Z. thank the Robert A. Welch Foundation (E-621) and the National Science Foundation (CHE-0714751) for support.

REFERENCES

(1) Cockrell, G. M.; Zhang, G.; VanDerveer, D. G.; Thummel, R. P.; Hancock, R. D. *J. Am. Chem. Soc.* **2008**, *130*, 1420.
(2) Petit, L.; Adamo, C.; Maldivi, P. *Inorg. Chem.* **2006**, *45*, 8517.
(3) Lewis, F. W.; Harwood, L. M.; Hudson, M. J.; Drew, M. G. B.; Desreux, J. F.; Vidick, G.; Bouslimani, N.; Modolo, G.; Wilden, A.; Sypula, M.; Vu, T.-H.; Simonin, J. P. *J. Am. Chem. Soc.* **2011**, *133*, 13093.
(4) Diamond, R. M.; Street, K.; Seaborg, G. T. *J. Am. Chem. Soc.* **1954**, *76*, 1461.
(5) Musikas, C. *Inorg. Chim. Acta* **1987**, *140*, 197.
(6) Cram, D. J.; Cram, J. M. *Acc. Chem. Res.* **1978**, *11*, 49.

(7) Hamilton, J. M.; Whitehead, J. R.; Williams, N. J.; Thummel, R. P.; Hancock., R. D. *Inorg. Chem.* **2011**, *50*, 3785−3790.
(8) Hamilton, J. M.; Anhorn, M. J.; Oscarson, K. A.; Reibenspies, J. H.; Hancock, R. D. *Inorg. Chem.* **2011**, *50*, 2764−2770.
(9) Hancock, R. D.; Martell, A. E. *Chem. Rev.* **1989**, *89*, 1875.
(10) Hancock, R. D.; Nikolayenko, I. V. *J. Phys. Chem.* **2012**, *116*, 8572.
(11) Carolan, A. N.; Mroz, A. E.; Reibenspies, J. H.; Thummel, R. P.; Hancock, R. D. in preparation.
(12) Littmann, G.; Thummel, R. P.; Hancock, R. D. in preparation.
(13) Martell, A. E.; Smith, R. M. *Critical Stability Constant Database, 46*; National Institute of Science and Technology (NIST): Gaithersburg, MD, 2003.
(14) Ballance, D. G.; Hancock, R. D., in preparation.
(15) Shannon, R. D. *Acta Crystallogr., Sect. A* **1976**, *A32*, 751.
(16) Shaffer, K. J.; McLean, T. M.; Waterland, M. R.; Wenzel, M.; Pileger, P. G. *Inorg. Chim. Acta* **2012**, *380*, 278.
(17) Wustefeld, H.-U.; Kaska, W. C.; Schuth, F.; Stucky, G. D.; Bu, X.; Krebs, B. *Angew. Chem., Int. Ed.* **2001**, *40*, 3182.
(18) Hancock, R. D. *Acc. Chem. Res.* **1990**, *23*, 253.
(19) Guillaumont, D. *J. Phys. Chem.* **2004**, *108*, 6893.
(20) Petit, L.; Joubert, L.; Maldivi, P.; Adamo, C. *J. Am. Chem. Soc.* **2006**, *128*, 2190.
(21) Hancock, R. D.; Bartolotti, L. J. *Inorg. Chem.* **2005**, *44*, 7175.
(22) Hancock, R. D.; Bartolotti, L. J. *Chem. Commun.* **2004**, 534.
(23) Hancock, R. D.; Bartolotti, L. J.; Kaltsoyannis, N. *Inorg. Chem.* **2006**, *45*, 10780.
(24) *Cambridge Structural Database*; Cambridge Crystallographic Data Centre: 12 Union Road, Cambridge CB2 1EZ, United Kingdom.
(25) Semenova, L. I.; White, A. H. *Aust. J. Chem.* **1999**, *52*, 539.
(26) Constable, E. C.; Elder, S. M.; Tocher, D. A. *Polyhedron* **1992**, *11*, 2599.
(27) Zong, R.; Zhang, G.; Eliseeva, S. V.; Bunzli, J.-C. G.; Thummel, R. P. *Inorg. Chem.* **2010**, *49*, 4657.
(28) Zong, R.; Thummel, R. P. *J. Am. Chem. Soc.* **2004**, *126*, 10800.
(29) Lyle, S. J.; Rahman, M. M. *Talanta* **1963**, *10*, 1177.
(30) Gabe, E. J.; Le Page, Y.; Charland, J.-P.; Lee, F. L.; White, P. S. *J. Appl. Crystallogr.* **1989**, *22*, 384.
(31) *ORTEP-3 for Windows*, Version 1.08; Farrugia, L. J. *J. Appl. Crystallogr.* **1997**, *30*, 565.
(32) Billo, E. J. *EXCEL for Chemists*; Wiley-VCH: New York, 2001.
(33) *HyperChem program*, version 8.0; Hypercube, Inc.:, Waterloo, Ontario, Canada.
(34) Hancock, R. D. *Prog. Inorg. Chem.* **1989**, *37*, 187.
(35) Schmidt, M. W.; Baldridge, K. K.; Boatz, J. A.; Elbert, S. T.; Gordon, M. S.; Jensen, J. H.; Koseki, S.; Matsunaga, N.; Nguyen, K. A.; Su, S.; Windus, T. L.; Dupuis, M.; Montgomery, J. A. *J. Comput. Chem.* **1993**, *14*, 1347.
(36) Lee, C.; Yang, W.; Parr, R. G. *Phys. Rev. B* **1988**, *37*, 785.
(37) Becke, A. D. *J. Chem. Phys.* **1993**, *98*, 5648.
(38) Weigend, F.; Ahlrichs, R. *Phys. Chem. Chem. Phys.* **2005**, *7*, 3297.
(39) Cundari, T. R.; Stevens, W. J. *J. Chem. Phys.* **1993**, *98*, 5555.
(40) Miguirditchian, M.; Guillaneuz, D.; Francois, N.; Airvault, S.; Ducros, S.; Thauvin, D.; Madic, D.; Illemassène, M.; Lagarde, G.; Krupa, J.-C. *Nucl. Sci. Eng.* **2006**, *153*, 223.
(41) Carolan, A. N.; Hancock, R. D. to be published.
(42) Bondi, A. *J. Phys. Chem.* **1964**, *68*, 441.
(43) Fedosseev, A. M.; Grigoriev, M. S.; Budantseva, N. A.; Guillaumont, D.; Le Naour, C.; Simoni, E.; Den Auwer, C.; Moisy, P. *C. R. Chim.* **2010**, *13*, 839.
(44) Mulla, F.; Marsicano, F.; Nakani, B. S.; Hancock, R. D. *Inorg. Chem.* **1985**, *24*, 3076.
(45) Janiak, C. *J. Chem. Soc., Dalton Trans.* **2000**, 3885.
(46) Dell'Amico, D. B.; Calderazzo, F.; Curiardi, M.; Labella, L.; Marchetti, F. *Inorg.Chem.* **2004**, *43*, 5459.
(47) Rogers, R. D.; Bond, A. H.; Aguinaga, S.; Reyes, A. *J. Am. Chem. Soc.* **1992**, *114*, 2967.
(48) R. Luckay, R.; Cukrowski, I.; Mashishi, J.; Reibenspies, J. H.; Bond, A. H.; Rogers, R. D.; Hancock, R. D. *J. Chem. Soc., Dalton Trans.* **1997**, 901.
(49) Garcia-Montalvo, V.; Cea-Olivares, R.; Williams, D. J.; Espinosa-Perez, G. *Inorg. Chem.* **1996**, *35*, 3948.
(50) Hancock, R. D.; Shaikjee, M. S.; Dobson, S. M.; Boeyens, J. C. A. *Inorg. Chim. Acta* **1988**, *154*, 229.
(51) Harrowfield, J. M.; Miyamae, H.; Shand, T. M.; Skelton, B. W.; Soudi, A. A.; White, A. H. *Aust. J. Chem.* **1996**, *49*, 1051.
(52) Shimoni-Livny, L.; Glusker, J. P.; Bock, C. P. *Inorg. Chem.* **1998**, *37*, 1853.
(53) Hancock, R. D.; Reibenspies, J. H.; Maumela, H. *Inorg. Chem.* **2004**, *43*, 2981.
(54) Cordero, B.; Gómez, V.; Platero-Prats, A. E.; Revés, M.; Echeverría, J.; Cremades, E.; Barragán, F.; Alvarez, S. *Dalton Trans.* **2008**, 2832.
(55) Kepert, D. L.; Waters, A. F.; White, A. H. *Aust. J. Chem.* **1996**, *49*, 117.